Supplementary Information (SI) for Materials Horizons.

Electronic Supplementary Information

Structural amine-induced interfacial electrical double layers for efficient photocatalytic H2 evolution

Jing Deng[a,b,#], Xinyu Xu[a,b,#], Bo Su[a,b], Minghui Liu[c,*], Xue Feng Lu[a,b], Wandong Xing[a,b,*], Zhian Lan[a,b], Guigang Zhang[a,b], and Sibo Wang[a,b,*]

[a] *State Key Laboratory of Chemistry for NBC Hazards Protection, College of Chemistry, Fuzhou University, Fuzhou 350116, China.*

[b] State Key Laboratory of Photocatalysis on Energy and Environment, College of Chemistry, Fuzhou University, Fuzhou 350116, China.

[c] College of Chemistry and Materials, Jiangxi Normal University, Nanchang, Jiangxi 330022, China.

Experimental Procedures

Materials

Ethanol (anhydrous, 99.7%), Sodium sulfide nonahydrate ($Na_2S \cdot 9H_2O$), Sodium sulfite (Na_2SO_3) and thiourea (CH_4N_2S) were provided from Sinopharm Chemical Reagent Co., Ltd. Cadmium acetate dihydrate ($Cd(Ac)_2 \cdot 2H_2O$) and diethylenetriamine ($C_4H_{13}N_3$, 99%) was purchased from Aladdin. Chloroplatinic acid solution (H_2PtCl_6) was purchased from Adamas. All the chemicals from commercial source were used without further purification.

Synthesis of CdS-D

0.9 mmol $Cd(Ac)_2 \cdot 2H_2O$ were added into 10.5 mL of water. Then, 42 mL of diethlenetriamine (DETA) and 2.25 mmol of thiourea were added. The mixture solution was transferred into Teflon-lined autoclave and kept the temperature at 180 °C for 10 h. Finally, the product was washed for three times with water and alcohol, respectively. After dying at 70 °C, CdS-D was obtained.

Synthesis of CdS

CdS was obtained by hydrothermal treatment on CdS-D. Specifically, 100 mg CdS-DETA and 60 ml water were added into 100 ml Teflon-lined stainless-steel autoclave. The sealed reactor was then placed in an oven and maintained at 180 °C for 10 h. After natural cooling, the obtained precipitation was washed for three times with water and alcohol, respectively. Then, the product was dried at 70 °C. Finally, CdS was obtained.

Synthesis of Pt/CdS-D

100 mg of CdS-D was dispersed in 10 mL deionized water and 1 ml TEOA, after sonicated for 10 min, 0.105 mL chloroplatinic acid solution (H_2PtCl_6, 9.52 mg/mL) was added into the suspension under stirring, and the mixture was illuminated by a xenon lamp for 30 min to deposit Pt NPs on CdS-D. The products were centrifuged and washed with deionized water for three times. After drying the sediment at 60 °C overnight, Pt/CdS-D composite was obtained.

Synthesis of Pt/CdS

For the synthesis of Pt/CdS, the synthesis procedure is quite similar to that of Pt/CdS-D. The only difference is the replacement of CdS-D, respectively.

Characterization

The crystal structures of samples were recorded on Bruker D8 Advance instrument with Cu Kα1 radiation (k = 1.5406 Å). The morphology, structure and composition of the samples were studied by Transmission electron microscopy (TEM), high-resolution transmission electron microscopy (HRTEM), energy dispersive X-ray (EDX) element mappings and EDX linear element scans on a FEI TECNAI G2F30 S-TWIN instrument at an accelerating voltage of 300 kV. X-Ray photoelectron spectra (XPS) and ultraviolet photoelectron spectroscopy (UPS) were examined on a Thermo Scientific ESCALAB 250 instrument with a monochromatized Al Kα line source (200 W). UV-vis diffuse reflectance spectra (DRS) were performed on a Varian Cary 500 UV-Vis-NIR spectrometer with an integrating sphere and $BaSO_4$ as a reflectance. The C 1s peak at 284.6 eV was referred in the data processing of all relevant elements. In situ room temperature photoluminescence (PL) spectra and time-resolved PL spectra were acquired on an Edinburgh Analytical Instruments FI/FSTCSPC 920, the excitation wavelength is 360 nm, and the lifetime was calculated as followed:

$$\tau = \frac{B_1\tau_1^2 + B_2\tau_2^2 + B_3\tau_3^2}{B_1\tau_1 + B_2\tau_2 + B_3\tau_3}$$

The nitrogen adsorption-desorption isotherms (77 K) and CO_2 adsorption isotherms (273 K) were collected on a Micromeritics ASAP 2020 surface area and porosity analyzer. The surface functional groups and reaction intermediates during the photocatalytic CO_2 reduction reaction were examined by Fourier transform infrared spectra (FTIR) and in situ diffuse reflectance infrared Fourier transform spectra (DRIFTS) with a Nicolet Magna 670 FTIR spectrometer, respectively. The electrical conductivity of samples was identified by electrochemical impedance spectra (EIS).

Electrochemical measurements: The electrochemical measurements were carried out on a BAS Epsilon Electrochemical System with a conventional three electrode cell including Pt plate as the counter electrode, Ag/AgCl electrode as the reference electrode and the as-prepared samples modified on FTO glass as the working electrode, respectively.

AQE measurement: The AQE was measured using a closed gas circulation and evacuation system and monochromatic visible light (395±5.0 nm). Depending on the amounts of H_2 gases produced by the photocatalytic reaction in an average of one hour, and the AQY was calculated as follow:

$$\eta_{AQE} = \frac{N_e}{N_p} \times 100\% = \frac{2 \times M \times N_A}{\frac{E_{total}}{E_{photon}}} \times 100\% = \frac{2 \times M \times N_A}{\frac{S \times P \times t}{h \times \frac{c}{\lambda}}} \times 100\% = \frac{2 \times M \times N_A \times h \times c}{S \times P \times t \times \lambda} \times 100\%$$

Where, M is the amount of H_2 molecules (mol), N_A is Avogadro constant ($6.022*10^{23}$ mol^{-1}), h is the Planck constant ($6.626*10^{-34}$ J·s), c is the speed of light ($3*10^8$ $m·s^{-1}$), S is the irradiation area (cm^2), P is the intensity of irradiation light ($W·cm^{-2}$), t is the photoreaction time (s), λ is the wavelength of the monochromatic light (m).

Photocatalytic H_2 reduction evaluation

The photocatalytic H_2 evolution reaction was carried out in closed quartz vessel equipped with Labsolar-6A all-glass automatic online trace gas analysis system (Perfectlight, Beijing). Typically, 10 mg photocatalyst was dispersed in 0.35 M Na_2S and 0.25 M Na_2SO_3 mixed solution (100 mL). Then, the system was stirred and under vacuum for 20 min. The temperature of the reaction was maintained at 10℃ using a circulating condensing unit. The light source was a 50 W 395 nm LED lamp. Lastly, the amount of H_2 was determined by Agilent 7820A gas chromatography (GC) equipped with a thermal conductive detector (TCD) and a 5 Å molecular sieve column, using the Ar as carrier gas. Other reaction conditions were the same as those of the typical reaction.

DFT calculations

We employed the Vienna Ab-initio simulation package (VASP)[1] to perform the spin-polarized density functional theory (DFT) calculations within the generalized gradient approximation (GGA)[2] using the Perdew–Burke–Ernzerhof (PBE) formulation[3]. Chosen the projected augmented wave (PAW) potentials[4] to describe the ionic cores and take valence electrons into account using a plane wave basis set with a kinetic energy cutoff of 450 eV. The electronic energy was considered self-consistent when the energy change was smaller than 10^{-4} eV. Geometry optimization was considered convergent when the force change was smaller than 0.03 eV/Å. The equilibrium lattice constants of anatase CdS unit cell were optimized by using a 9×9×6 Monkhorst-Pack k-point grid for Brillouin zone sampling[5], to be a=b=4.194 Å and c=6.823 Å. The supercell of CdS(10-10) slab model was 16.775 Å × 20.468 Å × 30.000 Å and contained 72 Cd and 72 S atoms. The Brillouin zone was sampled using a gamma (1 × 1 × 1) point. The Pt nanoparticle contains 13 atoms.

The hydrogen absorption free energies were calculated with reference to the computational hydrogen electrode (CHE) proposed by Nørskov et al[6] as follows: $\Delta G_H = \Delta E_{ads} + \Delta E_{ZPE} - T\Delta S$, where ΔE_{ads}, ΔE_{ZPE}, and ΔS represent the adsorption energy, zero potential energy, and entropy, respectively. The zero-point contributions are essentially identical, yielding $\Delta G_H = \Delta E_{ads} + 0.3$ eV.[7]

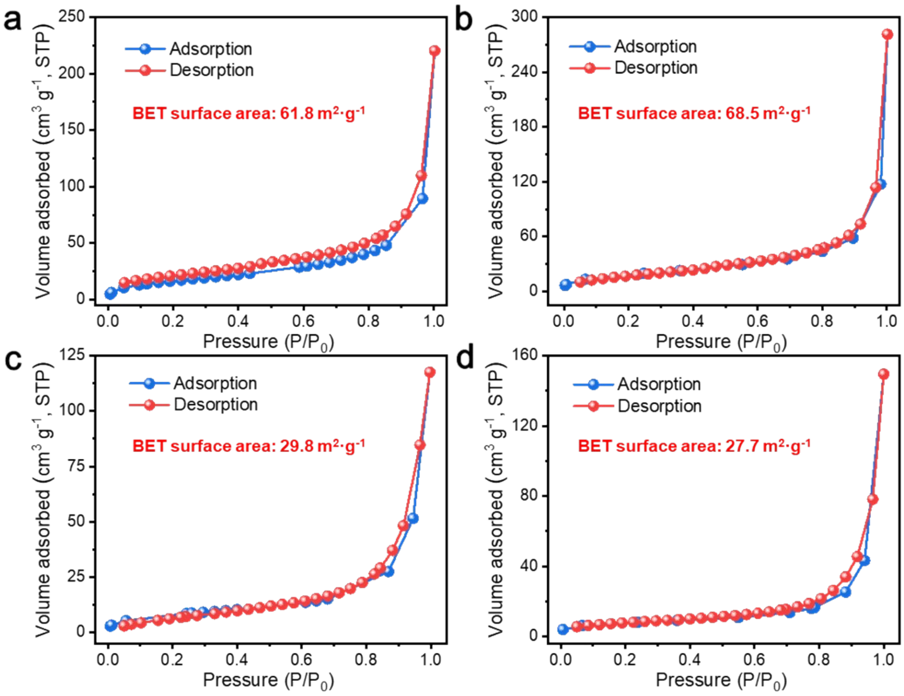

Figure S1. N_2 adsorption-desorption isotherms of (a) CdS-D, (b) Pt/CdS-D, (c) Pt/CdS and (d) CdS.

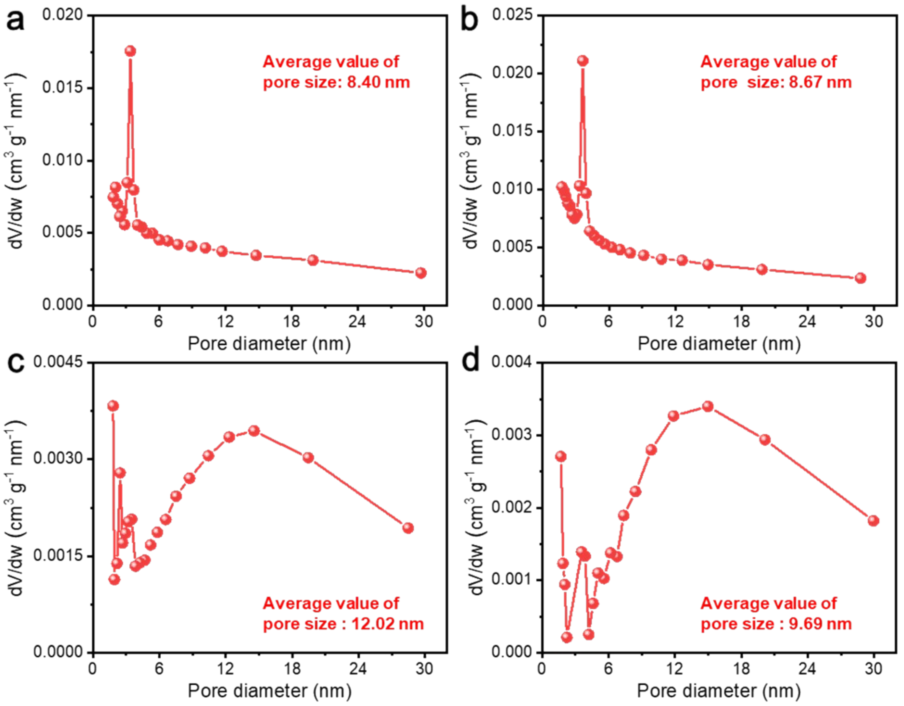

Figure S2. Pore size distribution plots of (a) CdS-D, (b) Pt/CdS-D, (c) Pt/CdS and (d) CdS.

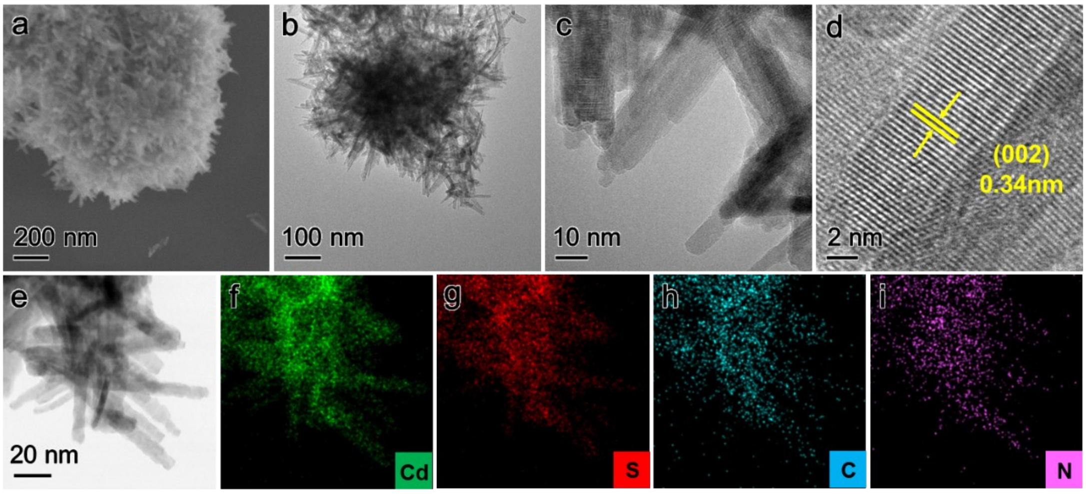

Figure S3. (a) SEM image, (b) TEM image, (c-d) HRTEM images, and (e-i) elemental mappings of CdS-D.

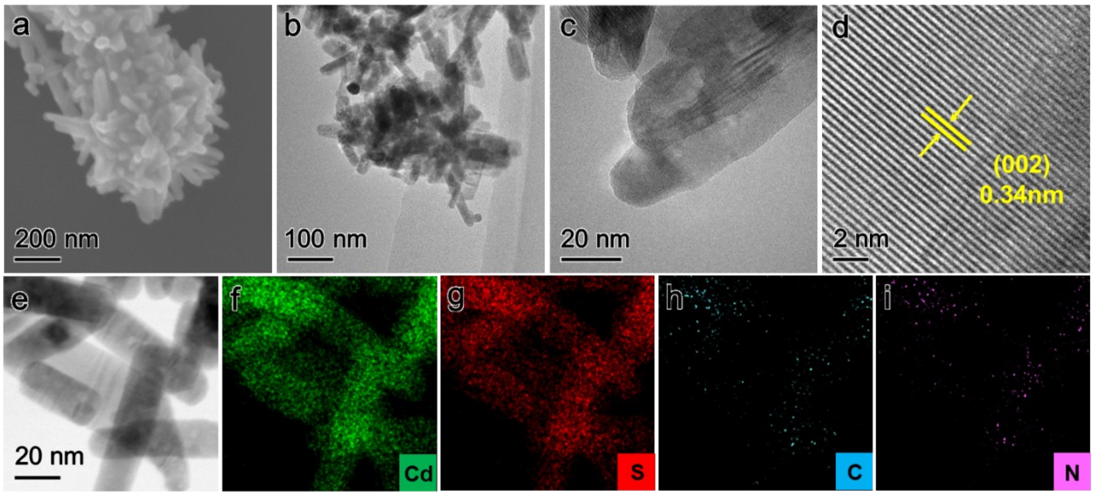

Figure S4. (a) SEM image, (b) TEM image, (c-d) HRTEM images, and (e-i) elemental mappings of CdS.

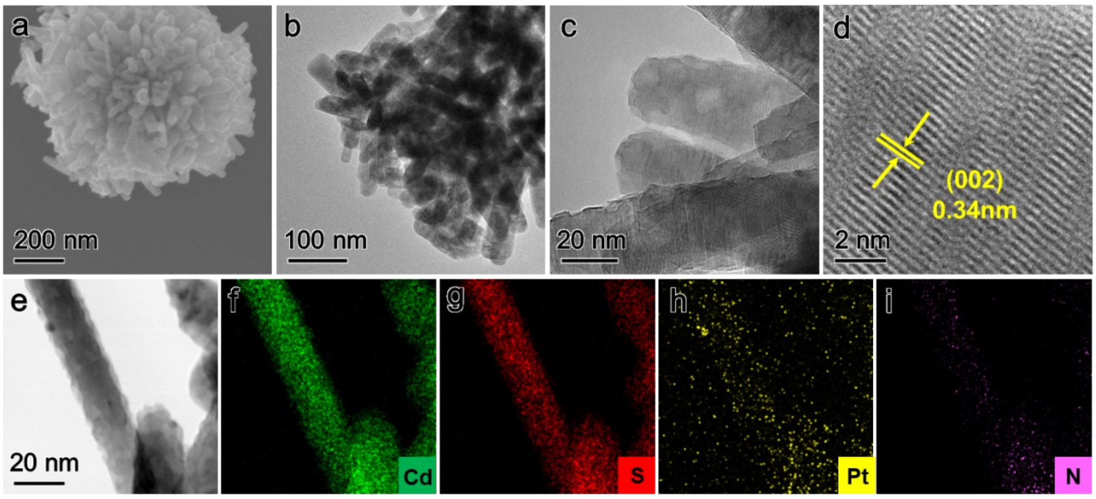

Figure S5. (a) SEM image, (b) TEM image, (c-d) HRTEM images, and (e-i) elemental mappings of Pt/CdS.

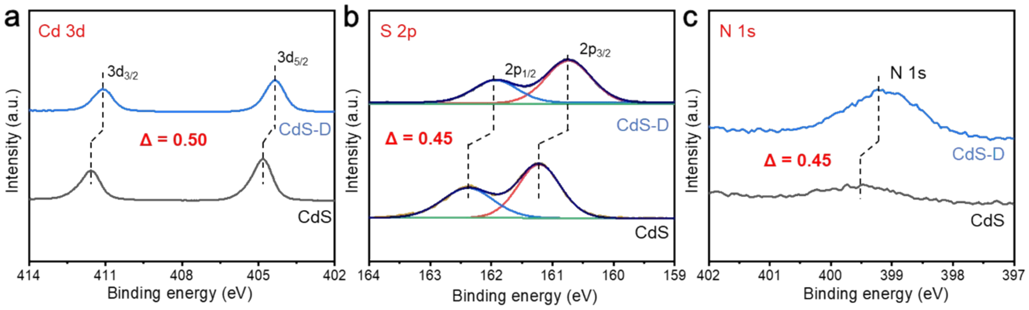

Figure S6. High resolution XPS spectra of (a) Cd, (b) S and (c) N of CdS-D and CdS.

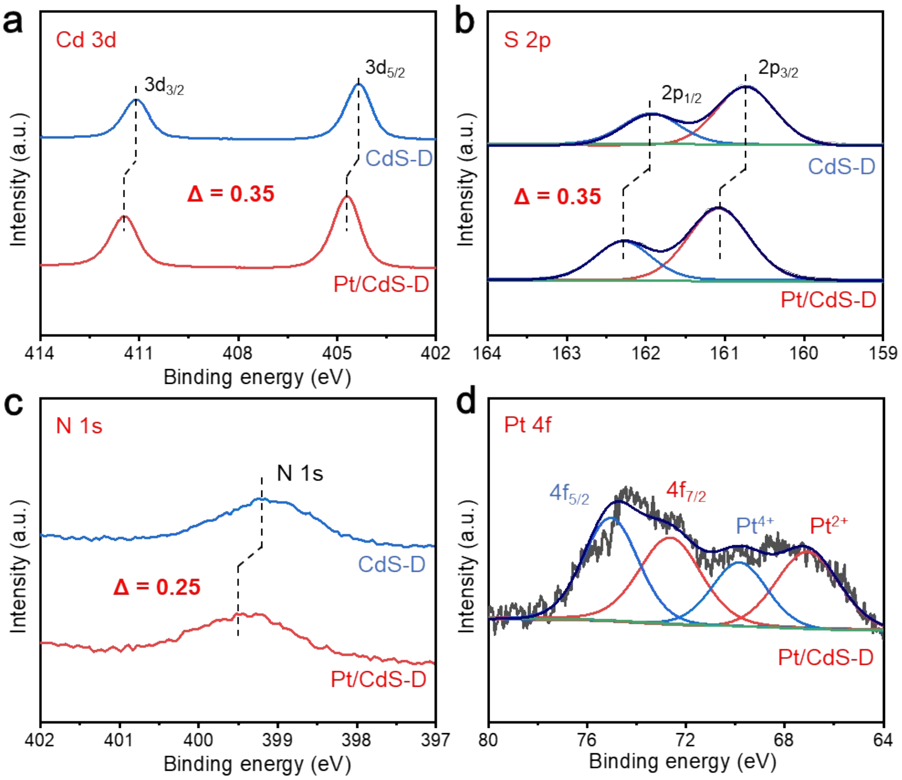

Figure S7. High resolution XPS spectra of (a) Cd, (b) S, (c) N and (d) Pt of CdS-D and Pt/CdS-D.

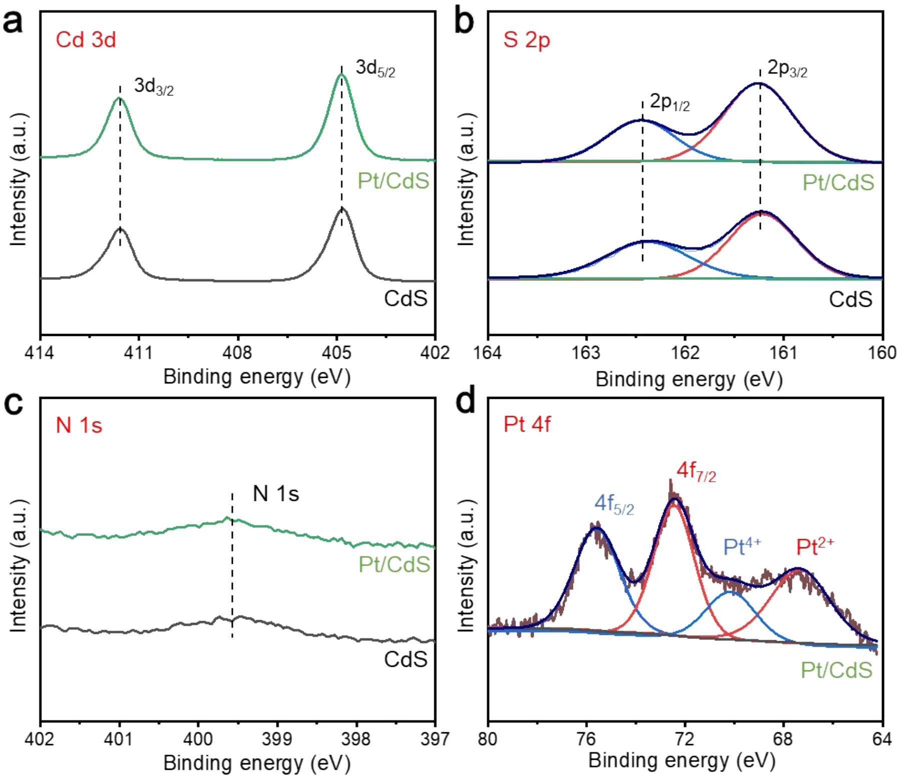

Figure S8. High resolution XPS spectra of (a) Cd, (b) S, (c) N and (d) Pt of CdS and Pt/CdS.

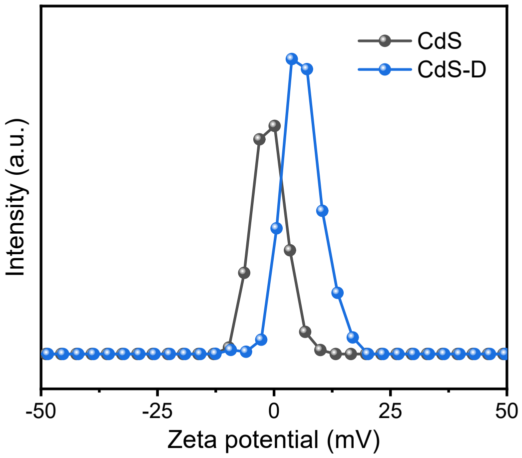

Figure S9. Zeta potential obtained in dispersion system using H_2O as medium.

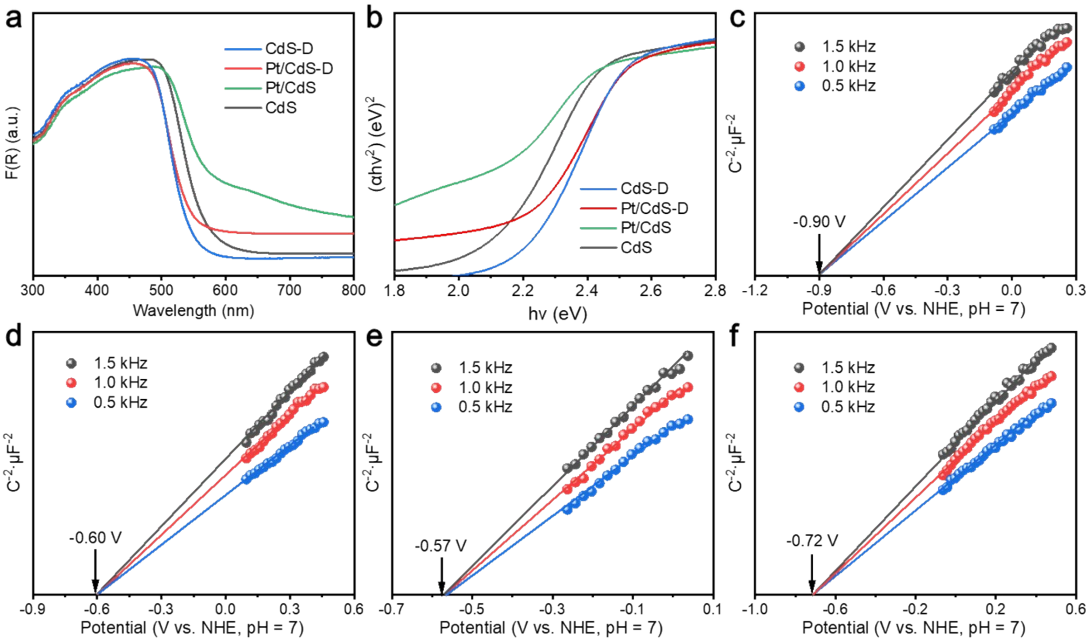

Figure S10. (a) UV-Vis absorption spectra and (b) Tauc plots of CdS-D, Pt/CdS-D, Pt/CdS and CdS. Mott-Schottky curves of (c) CdS-D, (d) Pt/CdS-D, (e) Pt/CdS and (f) CdS.

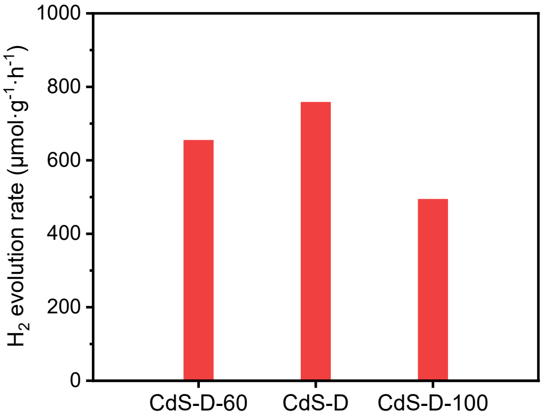

Figure S11. Photocatalytic H_2 evolution activities of CdS-D-60, CdS-D and CdS-D-100.

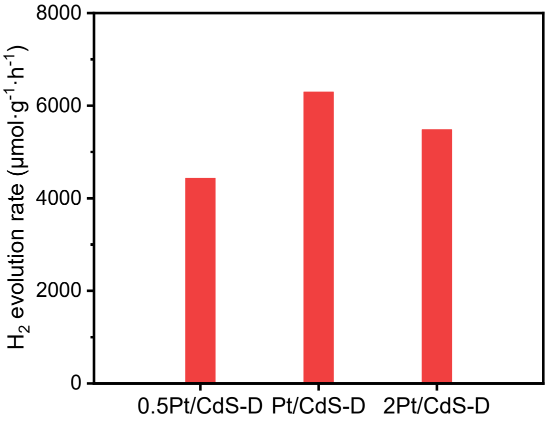

Figure S12. Photocatalytic H_2 evolution activities of 0.5Pt/CdS-D, Pt/CdS-D and 2Pt/CdS-D.

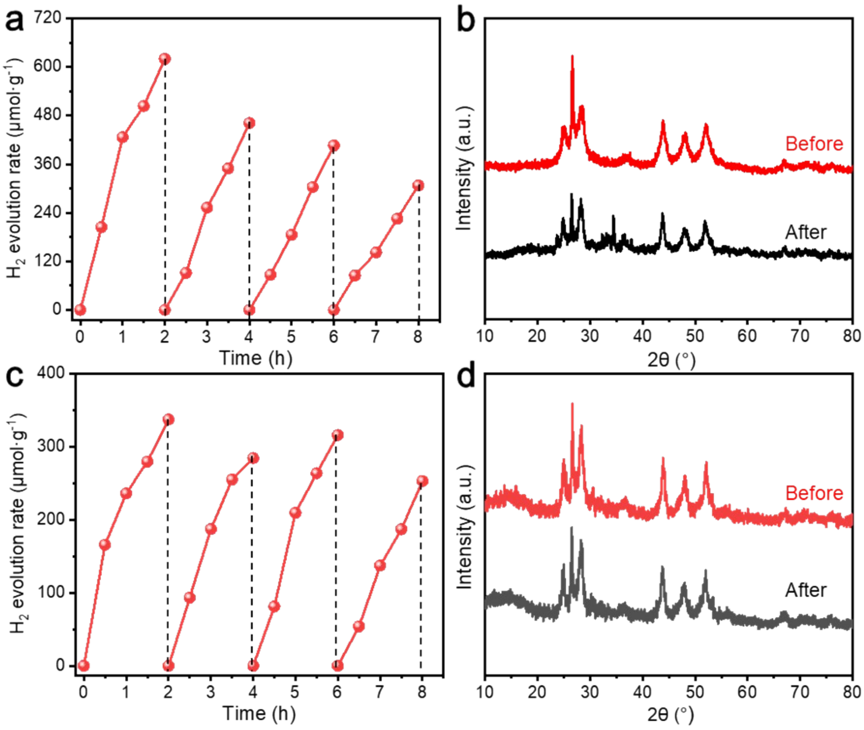

Figure S13. (a) Cycle test of Pt/CdS and (b) XRD of the used catalysts. (c) Cycle test of CdS and (d) XRD of the used catalysts.

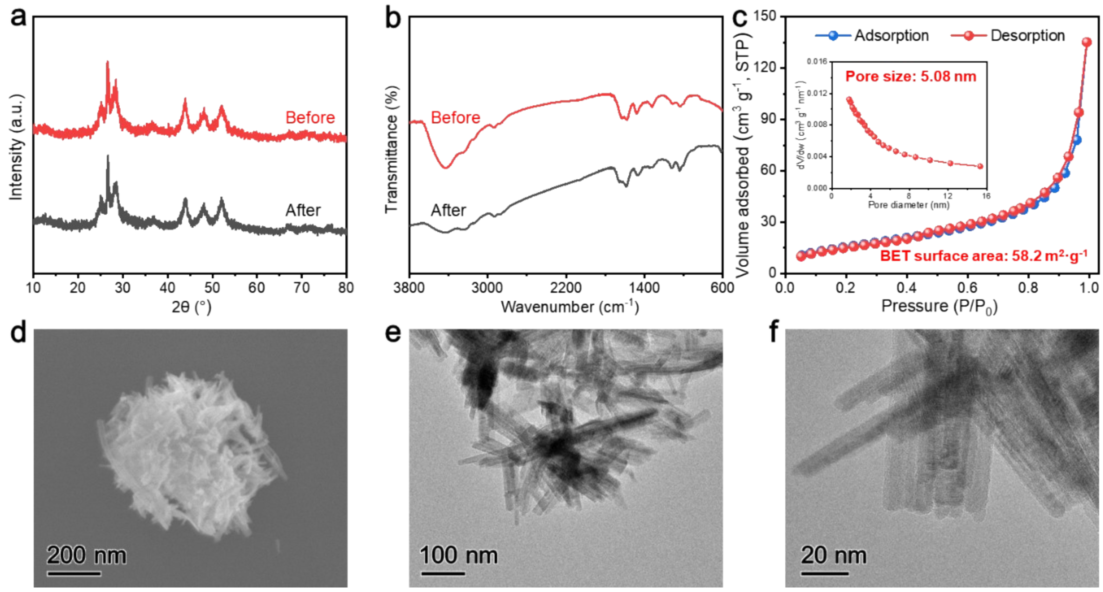

Figure S14. (a) XRD, (b) FTIR, (c) N_2 physisorption isotherms and pore size distribution plots (inset), (d) SEM, and (e-f) HRTEM of the used Pt/CdS-D after the cycling tests.

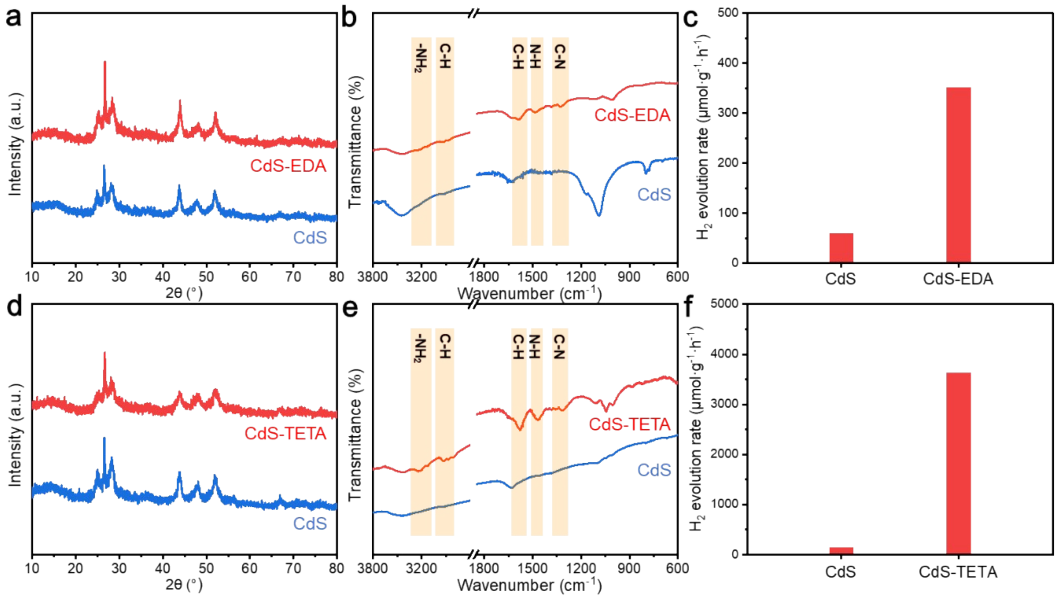

Figure S15. (a) XRD patterns, (b) FT-IR spectra and (c) Photocatalytic H_2 evolution activities of CdS and CdS-EDA. (d) XRD patterns, (e) FT-IR spectra and (f) Photocatalytic H_2 evolution activities of CdS and CdS-TETA.

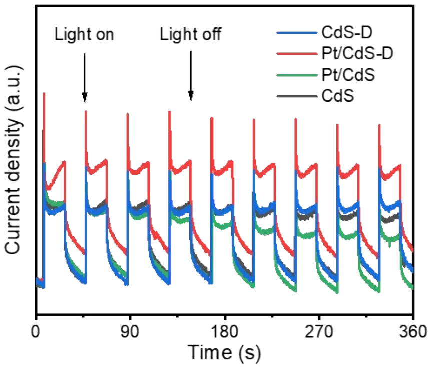

Figure S16. Transient photocurrent spectra of CdS-D, Pt/CdS-D, Pt/CdS and CdS.

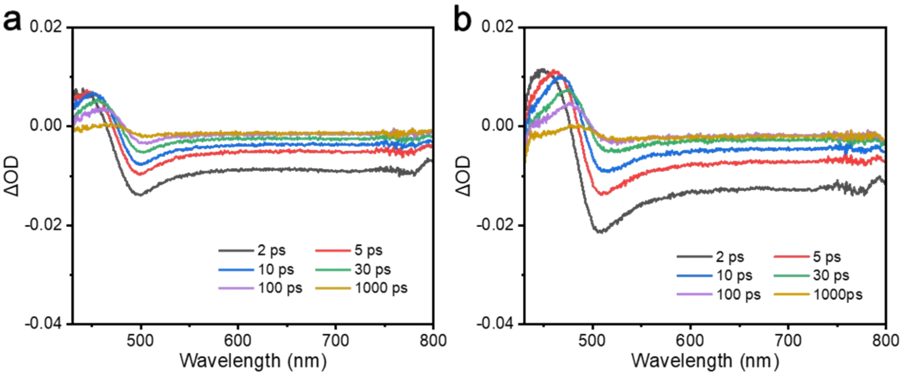

Figure S17. The decay signals transient absorption signals of of (a) CdS-DETA and (b) CdS monitored at 732 nm.

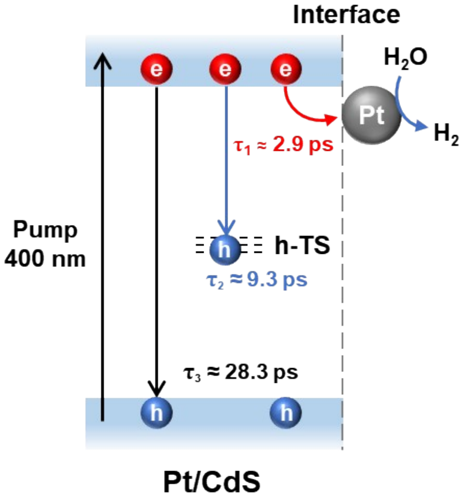

Figure S18. The schematics for electron quenching in Pt/CdS.

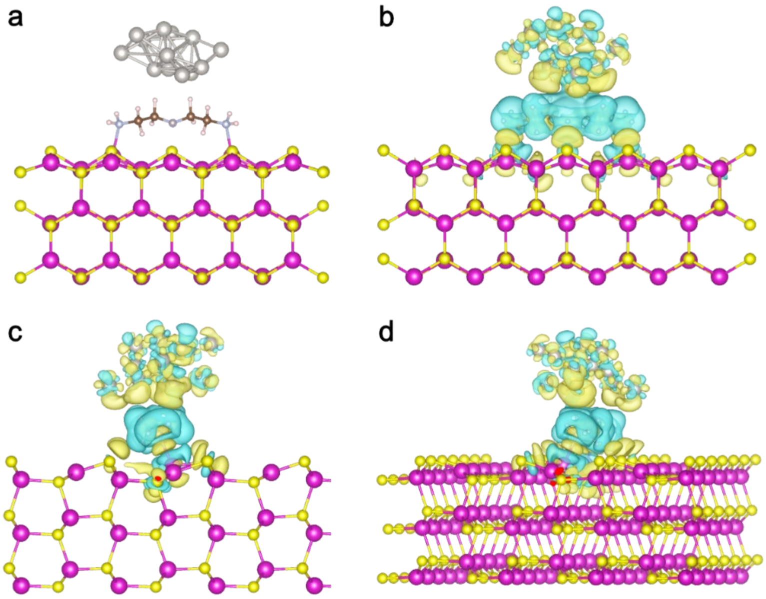

Figure S19. (a) Structural model of Pt/CdS-D and (b-d) Different perspectives of charge density difference diagram of Pt/CdS-D, where cyan indicates that the charge density decreases and yellow indicates that it increases.

Table S1. Band gap of CdS, Pt/CdS, CdS-D and Pt/CdS-D.

Sample	E_g (eV)
CdS	2.24
Pt/CdS	1.75
Pt/CdS-D	2.00
CdS-D	2.30

Table S2. Performance comparison of Pt/CdS-D with other reported catalysts about sulphide for H_2 production.

Catalyst	Light (nm)	Sacrificial reagent	Rate (umol h^{-1} g^{-1})	Refs.
$CuInS_2@C_3N_4$	350 W Xe lamp ($\lambda > 420$ nm)	TEOA	373	[8]
$CoFe_2O_4/ZnIn_2S_4$	250 W Xe lamp ($\lambda > 420$ nm)	TEOA	800	[9]
CdS/Co_3S_4	300 W Xe lamp ($\lambda > 420$ nm)	lactic acid	1084	[10]
NiO/CdS	300 W Xe lamp ($\lambda > 420$ nm)	Na_2S/Na_2SO_3	1300	[11]
ZIS-S/CNTs/RP	300 W Xe lamp	Na_2S/Na_2SO_3	1634	[12]
CdS NS@Ti_3C_2	300 W Xe lamp	methanol	1730	[13]
CdS/Mo-VC	300 W Xe lamp ($\lambda > 420$ nm)	lactic acid	2267	[14]
$CdS-MoS_2$	300 W Xe lamp ($\lambda > 420$ nm)	Na_2S/Na_2SO_3	2300	[15]
$Cr_{0.5}Ti_{0.5}N/CdS$	300 W Xe lamp ($\lambda > 420$ nm)	lactic acid	2440	[16]
CP/GDY	5W LED lamp	lactic acid	3765	[17]
$Pt_1/Cu-ZnIn_2S_4$	300 W Xe lamp ($\lambda > 420$ nm)	Na_2S/Na_2SO_3	5020	[18]

$CdS@Cd_xZn_{1-x}S$	300 W Xe lamp (λ > 420 nm)	Na_2S/Na_2SO_3	5170	[19]
CdS@POM	300 W Xe lamp (λ > 420 nm)	Na_2S/Na_2SO_3	5700	[20]
$CdS/ZnIn_2S_4$	300 W Xe lamp (λ =350-780 nm)	TEOA	5800	[21]
Pt/CdS-D	50W 395nm LED lamp	Na_2S/Na_2SO_3	6295	This work

Table S3. Fit results of the TRPL decay curves of CdS, Pt/CdS, Pt/CdS-D and CdS-D.

Sample	t (ns)
CdS	4.36
Pt/CdS	4.62
Pt/CdS-D	9.79
CdS-D	8.30

Table S4. Fitting parameters for the GSB peaks of Pt/CdS-D and Pt/CdS.

Sample	A_1	t_1	A_2	t_2	A_3	t_3	t_{ave}
Pt/CdS-D	0.65	2.72	0.34	30.29	0.12	457.66	379.95
Pt/CdS	0.71	2.93	0.29	9.31	0.21	28.27	18.57

1 G. Kresse and J. Furthmüller, *PRB*, 1996, **54**, 11169-11186.

2 J. P. Perdew, K. Burke and M. Ernzerhof, *Phys. Rev. Lett.*, 1996, **77**, 3865-3868.

3 J. P. Perdew, M. Ernzerhof and K. Burke, *JCP*, 1996, **105**, 9982-9985.

4 G. Kresse and D. Joubert, *PRB*, 1999, **59**, 1758-1775.

5 H. J. Monkhorst and J. D. Pack, *PRB*, 1976, **13**, 5188-5192.

6 J. K. Nørskov, J. Rossmeisl, A. Logadottir, L. Lindqvist, J. R. Kitchin, T. Bligaard and H. Jónsson, *J. Phys. Chem. B*, 2004, **108**, 17886-17892.

7 C. Zhou, J. Gao, Y. Deng, M. Wang, D. Li and C. Xia, *Nat. Commun*, 2023, **14**, 3592.

8 J. Luo, Z. Lin, Y. Zhao, S. Jiang and S. Song, *Chinese J Catal*, 2020, **41**, 122-130.

9 C. Li, H. Che, P. Huo, Y. Yan, C. Liu and H. Dong, *J. Colloid Interface Sci.*, 2021, **581**, 764-773.

10 F. Zhang, H.-Q. Zhuang, J. Song, Y.-L. Men, Y.-X. Pan and S.-H. Yu, *Appl. Catal. B Environ.*, 2018, **226**, 103-110.

11 L. Wei, D. Zeng, Z. Xie, Q. Zeng, H. Zheng, T. Fujita and Y. Wei, *Front Chem*, 2021, **9**.

12 L. Liu, J. Liu, W. Yang, J. Wan, F. Fu and D. Wang, *J. Colloid Interface Sci.*, 2022, **608**, 482-492.

13 X. Chen, Y. Guo, R. Bian, Y. Ji, X. Wang, X. Zhang, H. Cui and J. Tian, *J. Colloid Interface Sci.*, 2022, **613**, 644-651.

14 Y. Lei, K. H. Ng, Y. Zhu, Y. Zhang, Z. Li, S. Xu, J. Huang, J. Hu, Z. Chen, W. Cai and Y. Lai, *Chem. Eng. J.*, 2023, **452**, 139325.

15 H. Liu, P. Tan, Y. Liu, H. Zhai, W. Du, X. Liu and J. Pan, *J. Colloid Interface Sci.*, 2022, **619**, 246-256.

16 X. Meng, W. Qi, W. Kuang, S. Adimi, H. Guo, T. Thomas, S. Liu, Z. Wang and M. Yang, *J. Mater. Chem. A*, 2020, **8**, 15774-15781.

17 Z. Liu, E. Cui, X. Wang and Z. Jin, *Chem. Eng. J.*, 2024, **486**, 150060.

18 L. Su, P. Wang, J. Wang, D. Zhang, H. Wang, Y. Li, S. Zhan and J. Gong, *Adv. Funct. Mater.*, 2021, **31**, 2104343.

19 S. Kai, B. Xi, Y. Wang and S. Xiong, *Chem. Eur. J*, 2017, **23**, 16653-16659.

20 W.-X. Shi, Z.-Y. Liu and Z.-M. Zhang, *Inorg. Chem. Front*, 2023, **10**, 4534-4543.

21 P. Li, M. Liu, J. Li, J. Guo, Q. Zhou, X. Zhao, S. Wang, L. Wang, J. Wang, Y. Chen, J. Zhang, Q. Shen, P. Qu and H. Sun, *J. Colloid Interface Sci.*, 2021, **604**, 500-507.